Carbohydrate Polymers 93 (2013) 753–760

Contents lists available at SciVerse ScienceDirect

Carbohydrate Polymers

journal homepage: www.elsevier.com/locate/carbpol

Inclusion of quinestrol and 2,6-di-*O*-methyl-β-cyclodextrin: Preparation, characterization, and inclusion mode

Da-Wei Wang[a], Can-Bin Ouyang[a], Qi Liu[b,*], Hao-Liang Yuan[c], Xiao-Hui Liu[a]

[a] *Key Laboratory of Integrated Pest Management in Crops, Ministry of Agriculture, Institute of Plant Protection, Chinese Academy of Agricultural Sciences, Beijing 100193, PR China*
[b] *Key Laboratory of Dryland Agriculture, Ministry of Agriculture, Institute of Environment and Sustainable Development in Agriculture, Chinese Academy of Agricultural Sciences, Beijing 100081, PR China*
[c] *Laboratory of Molecular Design and Drug Discovery, School of Basic Science, China Pharmaceutical University, Nanjing 210009, PR China*

ARTICLE INFO

Article history:
Received 7 October 2012
Received in revised form
29 November 2012
Accepted 5 December 2012
Available online 12 December 2012

Keywords:
Quinestrol
2,6-Di-*O*-methyl-β-cyclodextrin
Inclusion complex
Water solubility
Molecular modeling

ABSTRACT

An inclusion complex between chemosterilant quinestrol and 2,6-di-*O*-methyl-β-cyclodextrin (DM-β-CD) was prepared using the solution-ultrasonic method. A 1:1 stoichiometry was confirmed by elemental analysis. Analytical techniques such as UV–vis spectroscopy, Fourier transform infrared spectroscopy, differential scanning calorimetry, X-ray diffraction, and scanning electron microscopy were used to characterize the complex. Proton NMR and nuclear Overhauser effect spectroscopy results indicate that the hydroxyl end and alkynyl end of quinestrol was included in the DM-β-CD cavity, which agrees with the most predominant configuration optimized by molecular modeling. The water solubility of quinestrol was significantly increased through complexation with DM-β-CD. The DM-β-CD complexes can be used in the design of a novel formulation of quinestrol for rat control products in agriculture.

1. Introduction

Rodents have caused huge economic losses, particularly in agriculture, forestry, and animal husbandry. At present, chemical methods are primarily used to prevent and control rodents, but with limited efficacy. However, these chemicals have polluted the environment, endangered human and animal safety, and undermined the stability of ecosystems. These effects make these compounds unsatisfactory for long-term rodent control. None of the available rodenticides can be considered sustainable for rodent control (Liu et al., 2012). With the gradually increasing environmental awareness, anti-rat measures have transformed from the extermination of rodents to the control and reduction of the rodent population density, also called as fertility control. Fertility control is considered as a non-lethal and sustainable method of managing rodent populations (Singleton, Leirs, Hinds, & Zhang, 1999). Some synthetic hormones have been tested for rodent control (Marsh & Howard, 1970). Ethynyl estradiol 3-cyclopentyl ether (Quinestrol, Scheme 1a) is a stable estradiol homologue that can be stored in the adipose tissue and then gradually released. This hormone mainly inhibits the release of the gonadotropin-releasing hormone from the hypothalamus and thus inhibits follicle growth (Zhao et al., 2007). This compound is also used in hormone replacement therapy and occasionally in breast and prostate cancer treatment (Tang et al., 2010). Quinestrol has been commercially used not only as a contraceptive for humans, but also as a chemosterilant for wild rodents (Kroc & Mischler, 1972; Liang et al., 2006; Zhang et al., 2004). However, studies on quinestrol as a chemosterilant are significantly limited because of its low water solubility. Hence, the identification of a new nontoxic and efficient carrier for quinestrol is important in promoting its scientific research and field application.

Cyclodextrins (CDs) are nontoxic macrocyclic oligosaccharides consisting of (α-1,4)-linked α-L-glucopyranose units with a hollow hydrophobic interior and a hydrophilic outer surface. These compounds can form inclusion complexes with a wide variety of organic compounds, which enter partly or entirely into the relatively hydrophobic cavity of CDs and simultaneously expel the few high-energy water molecules from the interior (Karathanos, Mourtzinos, Yannakopoulou, & Andrikopoulos, 2007). This phenomenon usually enhances drug solubility in an aqueous solution and affects the chemical characteristics of the encapsulated drug in the pharmaceutical industry (Chen et al., 2011; Misiuk & Zalewska, 2009; Wu, Liang, Yuan, Wang, & Yan, 2010). However, natural CDs have limited water solubility, which negatively affects the water solubility of the formed complex. To address this problem, alkyl moieties such as hydroxyalkyl or methyl on free hydroxyl groups of β-CD were introduced. The complexing ability of CD derivatives

* Corresponding author. Tel.: +86 010 82109767; fax: +86 010 82105981.
E-mail address: liuqi@ieda.org.cn (Q. Liu).

0144-8617/$ – see front matter © 2013 Published by Elsevier Ltd.
http://dx.doi.org/10.1016/j.carbpol.2012.12.007

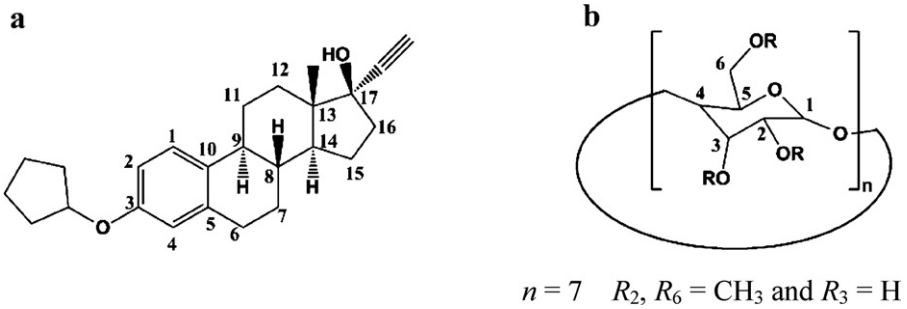

Scheme 1. Structures of ethynyl estradiol-3-cyclopentyl ether (a) and 2,6-di-*O*-methyl-β-cyclodextrin (b).

was significantly modified relative to the parents. For example, 2,6-di-*O*-methyl-β-cyclodextrin (DM-β-CD, Scheme 1b) shows higher affinity for various drugs as well as higher solubilizing ability compared with natural β-CD (Alcaro et al., 2002). The water solubility of four types of nitroindazole derivatives have been improved in neutral aqueous solutions through complexation with DM-β-CD (Pérez-Cruz, Jullian, Rodriguez, Arán, & Olea-Azar, 2009). This complexation induced a low permeation of WIN 51711 across excised bovine nasal mucosa with a latency of 2 h, thus allowing a topical action of the drug in the hours immediately following the application (Ventura et al., 2006).

Recently, we reported the inclusion complexation of HP-β-CD with the chemosterilant levonorgestrel. Our results showed that HP-β-CD increased the water solubility and enhanced the UV-stability of levonorgestrel (Wang, Liu, Liu, & Liu, 2011). As a continuation of our studies, an inclusion complex of quinestrol with DM-β-CD was investigated. To the best of our knowledge, no scientific study on this inclusion complex has been reported to date.

This work aims to improve the water solubility of quinestrol through complexation with DM-β-CD. The inclusion complex of quinestrol and DM-β-CD was prepared and systematically characterized using elemental analysis, ultraviolet–visible (UV–vis) spectroscopy, Fourier transform infrared spectroscopy (FT-IR), differential scanning calorimetry (DSC), X-ray diffraction (XRD), Proton NMR (^{1}H NMR) and two-dimensional nuclear magnetic resonance (2D NMR) spectroscopy, and scanning electron microscopy (SEM). The inclusion mode of the complex was obtained from both experimental and theoretical results. The solubilization effect of DM-β-CD on quinestrol was also investigated. This study aims to provide an efficient approach to developing new rodent chemosterilants with high water solubility and low toxicity.

2. Materials and methods

2.1. Materials

Quinestrol (FW = 364.50, purity > 99%) was obtained from Sigma–Aldrich (Dorset, UK). DM-β-CD (FW = 1331.39, PC > 99.5%) was purchased from Wako Pure Chemical Industries, Ltd. (Japan). Other reagents and chemicals were of analytical grade. All experiments were performed using ultrapure water.

2.2. Preparation of the quinestrol and DM-β-CD complex

A solution-ultrasonic method (Miecznik & Kaczmarek, 2007) was used to prepare the inclusion complex. Quinestrol (0.3 mM, 10.94 mg) and DM-β-CD (0.1 mM, 13.31 mg) were dissolved in a mixed solution of ethanol and water (10 ml, V:V = 1:4). The mixture was placed in an ultrasonic bath for 2 h at room temperature and in the dark to protect from degradation. After evaporating the reaction mixture, the obtain mixture was added with 10 ml water. The excess quinestrol was removed using a 0.45 μm hydrophilic membrane. The resulting solution was then lyophilized with an EYELA FD-81 freeze-drier at −80 °C (Tokyo Rikakikai, Japan) to obtain the powder. The resulting solid inclusion complex was then collected.

2.3. Preparation of the quinestrol and DM-β-CD physical mixture

To determine the possible structure of the inclusion, a physical mixture was prepared using a previously reported method (Yang, Lin, Chen, & Liu, 2009). In brief, a 1:1 molar mixture of quinestrol and DM-β-CD was ground with a small amount of water (the minimum amount to form a slurry) in a ceramic mortar for 3 min.

2.4. Standard curve of quinestrol

A series of quinestrol ethanol solutions with concentrations ranging from 20.00 mg/L to 240.0 mg/L were prepared. The measurements were performed using a UV–vis spectrophotometer (Shimadzu UV-2550, Japan) at 280 nm. A standard curve was then prepared using the concentrations (C, mg/L) as the x-coordinate and the absorbance (A) as the y-coordinate. The standard curve of quinestrol can be expressed by $A = 5.56C + 0.0017$ ($R^2 = 0.9999$).

2.5. Phase solubility test

Phase solubility studies were performed according to the methods described by Higuchi and Connors (Higuchi & Connors, 1965). Excess amounts of quinestrol was suspended in a 0.1 mol/L phosphate buffer solution (pH 7.0) containing increasing amounts of DM-β-CD (from 0 mM to 10.00 mM). The mixtures were placed in an ultrasonic bath for 2 h at 25 °C in the dark and were then left in the dark for 24 h. After equilibrium was reached, the mixtures were withdrawn and subsequently filtered through a 0.45 μm hydrophilic membrane filter. All samples were prepared in triplicate. The concentration of quinestrol in the filtrate was determined at 280 nm using a Shimadzu UV-2550 (Japan). The phase solubility profiles were obtained by plotting the solubility of quinestrol vs. the concentration of DM-β-CD. The apparent stability constant, K_C, of the quinestrol and DM-β-CD complex can be calculated from the slope and the intercept of the linear segment of the phase solubility line using the following equation:

$$K_C = \frac{k}{S_0(1-k)} \quad (1)$$

where S_0 is the intrinsic solubility of quinestrol in ultrapure water in the absence of DM-β-CD, and k is the slope of the straight line.

2.6. Characterization

2.6.1. Elemental analysis

The composition of the complex was determined by elemental analysis. The data were performed on a Flash EA 1112 elemental analyzer (Italy).

2.6.2. UV–vis spectra

UV–vis spectroscopy was conducted using a conventional 1 cm path (1 cm × 1 cm × 4 cm) quartz cell on a Shimadzu UV-2550 (Japan) at 25 °C. A water/ethanol (V:V = 4:1) solution (pH 7.0) was used because of the low water solubility of the drug. The quinestrol concentration was kept constant at 0.137 mM. An appropriate amount of DM-β-CD was then added to obtain final concentrations of 0, 2.50, 5.00, 7.50, 10.0 and 12.5 mM. UV spectroscopy was performed after 1 h in the spectral range of 200–400 nm.

2.6.3. FT-IR

The FT-IR spectra of quinestrol, DM-β-CD, their physical mixture, and the inclusion complex between 4000 cm^{-1} and 500 cm^{-1} (mid-infrared region) were obtained using a Bruker Tensor 27 FTIR spectrophotometer (Germany). Each sample was prepared with spectroscopic grade KBr *powder* and then pressed into 1 mm pellets (1 mg of sample per 100 mg dry KBr) using a press sheet.

2.6.4. DSC

Quinestrol, DM-β-CD, their physical mixture, and the inclusion complex were analyzed using DSC (Mettler Toledo DSC 822e, Switzerland). All samples were previously dried for 24 h at 105 °C. Each dried powder (3–5 mg) was heated in a crimped aluminum pan between 50 and 240 °C at a scanning rate of 5 °C/min and under a nitrogen flow of 40 ml/min. An empty pan sealed in the same manner was used as a reference. The reproducibility was verified by running the sample in triplicate.

2.6.5. XRD

The XRD patterns were obtained using a Rigaku D/Max-2500 V X-ray diffractometer (Japan) with Cu Kα radiation (40 kV, 200 mA) at a scanning rate of 10°/min. The powder samples were mounted on a vitreous sample holder and scanned between $2\theta = 3°$ and 60° at a step size of $2\theta = 0.02°$.

2.6.6. SEM

The surface morphologies of the samples were examined using a Hitachi s-4800 high-resolution SEM (Japan). The samples were prepared by mounting approximately 0.5 mg of powder onto a 5 mm × 5 mm silicon wafer prior to examination. The powder was then sputter-coated with gold particles, and the samples were examined using SEM at 5.0 or 15 kV.

2.6.7. ^1H and 2D NMR

The ^1H NMR spectra of DM-β-CD and the quinestrol/DM-β-CD inclusion complex were obtained using a Bruker ARX400 spectrometer at 298 K. Tetramethylsilane (TMS) was used as an internal standard. Chemical shifts (δ) are expressed in ppm relative to TMS. All samples were dissolved in 99.98% D_2O and filtered prior to use.

Two-dimensional (2D) nuclear Overhauser effect spectroscopic (NOESY) experiments were run on a Bruker ARX600 spectrometer. The samples were equilibrated for at least 24 h prior to the measurement. The NOESY spectra were acquired at 298 K with presaturation of the residual water resonance and at a mixing (spin-lock) time of 170 ms. The analyses were conducted at a 6 kHz field. All 2D NMR experiments were performed in D_2O.

2.7. Molecular modeling

2.7.1. Molecular docking

A Schrödinger suite 2009 software package was used for computational studies to verify the structure of the DM-β-CD and quinestrol complex. Three-dimensional structures of DM-β-CD and quinestrol were initially constructed on Maestro (Maestro, version 9.0, Schröinger, 2009). The structures were then manipulated using a MacroModel (MacroModel, version 9.7, Schröinger, 2009) module for energy minimization through a 5000-step Polak-Ribiere conjugate gradient, with OPLS-2005 as the force field and a GB/SA model as the solvation treatment. Docking was performed using the DM-β-CD centroid to center the enclosing box, which was used as the docking space, with the Glide (Glide, version 5.5, Schröinger, 2009) program. Quinestrol was then flexibly docked using the Glide extra precision mode. Finally, the optimum scoring pose of the inclusion modes was selected as output.

2.7.2. Energy calculation

The energy of the inclusion complexes in water was calculated with an MM3* force field using a MacroModel software. As the proportional stability of complex formation, the relative thermodynamic relationship was considered in the molecular mechanics calculations. According to de Jesus et al. (2006), the enthalpy of formation (ΔH_f) can be obtained from the MM calculations, which are proportional to the stability constant of the inclusion complex. ΔH can be calculated from the minimum energy structure according to

$$\Delta H = \Delta H_{f\,complex} - (\Delta H_{f\,Quinestrol} + \Delta H_{f\,DM\text{-}\beta\text{-}CD}). \quad (2)$$

3. Results and discussion

3.1. Phase solubility studies

Phase solubility studies have been extensively used in investigating the solubility of several drugs and agrochemicals in the presence of CDs (Rajabi, Tayyari, Salari, & Tayyari, 2008; Villaverde et al., 2004). A linear relationship between the amount of solubilized quinestrol and the DM-β-CD concentration in solutions was observed. This relationship was classified as a typical A_L-type. The stoichiometry of the quinestrol and DM-β-CD inclusion complex was then determined. The regression equation is as follows:

$$Y = 1.512 \times 10^{-4}X + 3.04 \times 10^{-5}, \quad R^2 = 0.994$$

where Y is the concentration (mM) of quinestrol and X is the concentration (mM) of DM-β-CD. According to Higuchi and Connors's theory (Higuchi & Connors, 1965), this condition may be attributed to the formation of a 1:1 inclusion complex between quinestrol and DM-β-CD.

According to Meylan's reports (Meylan, Howard, & Boethling, 1996), the calculated water solubility of quinestrol is 0.0378 mg/L. The calculated apparent stability constant of the quinestrol/DM-β-CD complex was $1.45 \times 10^3\ M^{-1}$ according to Eq. (1), suggesting that a favorable interaction generally occurs in the drug-CD association constants ranging from 50 M^{-1} to 2000 M^{-1} (Loftsson, Hreinsdóttir, & Másson, 2005). Compared with the solubility of quinestrol in ultrapure water in the absence of DM-β-CD, a 14.8-fold increase in the presence of 10.0 mM DM-β-CD was found.

According to the results of Pérez-Cruz et al.'s research (Pérez-Cruz et al., 2009), a 1:1 inclusion complex of NI and DM-β-CD was formed. In addition, the aqueous solubility of NI was improved in a neutral aqueous solution through complexation with DM-β-CD. Ventura et al. (2006) reported Ap-type diagrams at different temperatures, which imply the presence of two WIN 51711–DM-β-CD complexes in the solution at 1:1 and 1:2 molar ratios. The 1:1 complex formed more easily than the other one.

Table 1
Elemental analytical results for the inclusion complex of quinestrol and DM-β-CD.

Element	Calculated (1:1 complex) (%)	Found (%)
C	50.88	50.37
H	8.12	8.26

3.2. Characterization results and discussion

3.2.1. Elemental analysis

The analytical data for the elemental composition test on the inclusion complex are shown in Table 1. The composition and stoichiometry of the inclusion complex was confirmed by elemental analysis (He, Deng, & Yang, 2008). The results suggest that the molecular formula of the inclusion complex is $C_{56}H_{98}O_{35}\cdot C_{25}H_{32}O_2\cdot 12H_2O$, which indicates the formation of the inclusion complex of quinestrol and DM-β-CD at a 1:1 mole ratio. Twelve water molecules were also found in the inclusion complex. Xia et al. (Ge et al., 2011) reported that an inclusion complex can form between 6-benzylaminopurine and β-CD at a mole ratio of 1:1, and that eight water molecules are also found in the complex.

3.2.2. UV–vis spectral analysis

UV–vis spectroscopy is an important tool in the study of complexation (Lauro et al., 2012; Wang, Cao, Sun, & Wang, 2011). The inclusion behavior of DM-β-CD with quinestrol was investigated in a water/ethanol (V:V = 4:1) solution system because of the rather limited water solubility of quinestrol. No perceptible change in the pH of the solution was observed during the entire experiment. Fig. 1 shows that the spectrum of quinestrol exhibits a slight redshift. In addition, its absorbance intensity gradually increases with the stepwise addition of DM-β-CD, which may have been caused by the conjugation effect of the two compounds. In the spectrum of quinestrol in the aqueous solution without DM-β-CD, two λ_{max} values were found at 287.1 nm (π–π^* transition of the phenolic group) and 279.6 nm (π–π^* transition of the phenyl ring). However, the absorption maxima of the inclusion complex shifted to 280.6 and 288.3 nm, respectively, compared with that of quinestrol alone. Given that the size-, shape-, and charge-fit effects are the dominant controlling factors in the formation of inclusion complexes of CDs (Liu & Chen, 2006), these results indicate that the inclusion behavior mainly depends on the individual structural features of DM-β-CD and quinestrol.

All these results suggest that DM-β-CD can form an inclusion complex with quinestrol, indicating the possibility of interactions between quinestrol and DM-β-CD as a result of a partial shielding of quinestrol into the DM-β-CD cavity.

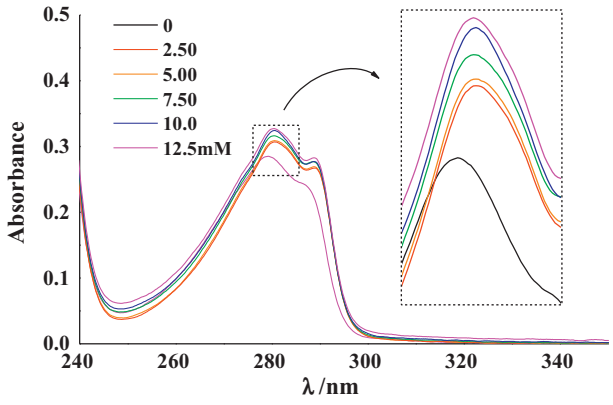

Fig. 1. Absorbance spectra of quinestrol (0.137 mM) and DM-β-CD (0, 2.50, 5.00, 7.50, 10.0, 12.5, 15.0, and 17.5 mM) at 25 °C, pH 7.0.

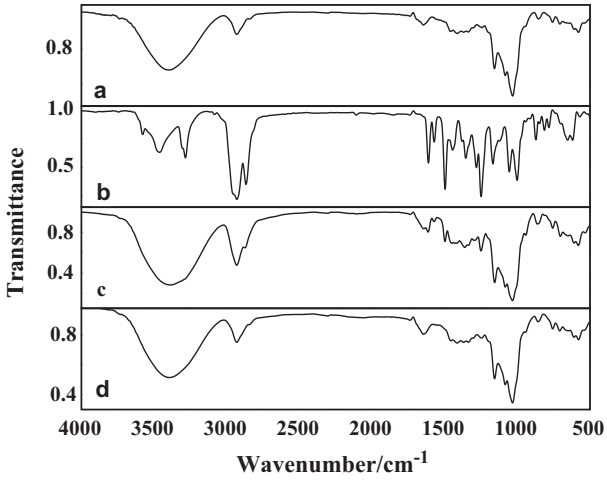

Fig. 2. Fourier transform infrared (FT-IR) spectra of (a) DM-β-CD, (b) quinestrol, (c) physical mixture of quinestrol and DM-β-CD, and (d) quinestrol and DM-β-CD inclusion complex at a 1:1 molar ratio.

3.2.3. FT-IR analysis

FT-IR was used to confirm the formation of an inclusion complex (Wang, Liu et al., 2011). The FT-IR spectra of DM-β-CD, quinestrol, their physical mixture, and the inclusion complex are shown in Fig. 2. The IR spectra of DM-β-CD (Fig. 2a) is characterized by the prominent band at 3397 cm^{-1} (for the O–H stretching vibrations) and 2931 cm^{-1} (for the C–H stretching vibrations), as well as by the 1154, 1085, and 1036 cm^{-1} bands (for C–H and C–O stretching vibrations). Meanwhile, the FT-IR spectrum of quinestrol (Fig. 2b) is characterized by several peaks. The absorption band of O–H was found at 3462 cm^{-1}. The C≡CH stretching vibrations are indicated by the sharp band at 3284 cm^{-1}. Another group of characterstic absorption peaks is that of the stretching vibration of the benzene ring skeleton at 1612, 1571, 1497, and 1444 cm^{-1}. The peak at 1249 cm^{-1} is attributed to the C–O–C asymmetric stretching vibration. Meanwhile, the spectra of the physical mixture correspond to the superposition of the spectra of the two individual components (Fig. 2c). However, not all of these characteristic bands are present in the spectra of the inclusion complex of quinestrol and DM-β-CD. A number of bands decreased and even disappeared in the new complex, most notably the C≡CH stretching vibrations. Compared with DM-β-CD, the spectral result of the inclusion complex exhibits a certain shift of the peak assigned to the O–H stretching vibrations from 3397 cm^{-1} to 3399 cm^{-1}.

All these phenomena indicate the formation of the inclusion complex. In addition, some parts of quinestrol were included into the DM-β-CD cavity, possibly the hydroxy and ethynyl ends.

3.2.4. DSC analysis

The thermal properties of quinestrol, DM-β-CD, their physical mixture, and the inclusion complex were investigated using DSC tests; the results are shown in Fig. 3. A broad endothermic peak (Fig. 3a) was observed at approximately 72 °C as a result of the amorphous nature of DM-β-CD. By contrast, quinestrol exhibited one sharp endothermic peak at 110 °C (Fig. 3b), which corresponds to the melting point of the drug's crystalline form. A similar phenomenon was observed for quinestrol in its physical mixture with DM-β-CD (Fig. 3c). The thermal profile shows the unchanged broad bands of DM-β-CD at 72 °C as well as a distinct melting peak, which has the same shape and melting temperature as pure quinestrol. However, a completely different pattern was obtained in the thermogram of the quinestrol and DM-β-CD inclusion complex

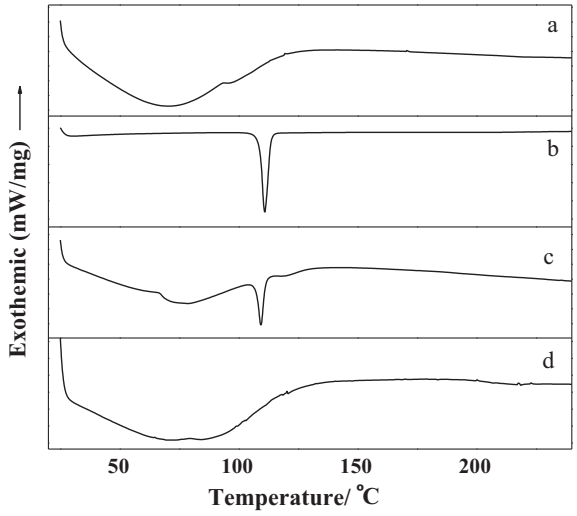

Fig. 3. Differential scanning calorimetric (DSC) thermograms of (a) DM-β-CD, (b) quinestrol, (c) physical mixture of quinestrol and DM-β-CD, and (d) quinestrol and DM-β-CD inclusion complex at a 1:1 molar ratio.

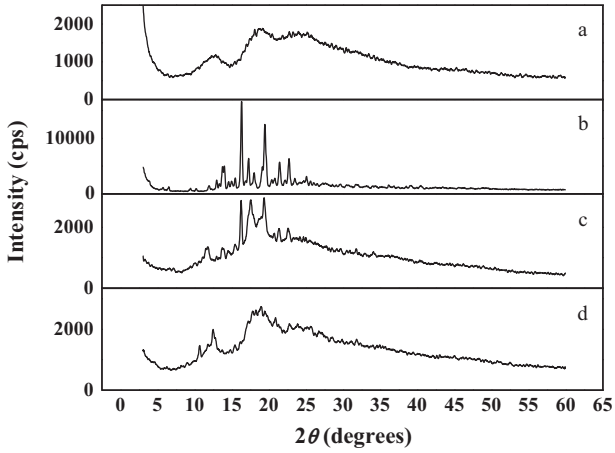

Fig. 4. X-ray diffraction (XRD) patterns of (a) DM-β-CD, (b) quinestrol, (c) physical mixture of quinestrol and DM-β-CD, and (d) quinestrol and DM-β-CD inclusion complex at a 1:1 molar ratio (d).

(Fig. 3d). The disappearance of the melting peak of quinestrol at 110 °C and the appearance of a new peak at 85 °C are indicative of an essential change in the substance structure as well as a strong interaction between the quinestrol and DM-β-CD of the inclusion complex.

These findings show that the solution-ultrasonication, along with the freeze-drying method, yields a new inclusion compound. However, no association occurs when the two powders are simply mixed together. Furthermore, the stability of quinestrol deteriorated after the inclusion complexation, which may be beneficial in reducing the risks of harmful organisms in the field.

3.2.5. XRD analysis

Powder XRD patterns allow the examination of the medium- and long-range ordering of materials (Correia et al., 2002). The diffraction pattern of the complex is assumed to be distinct from that of the superposition of each of the components if a true inclusion complex is formed (Veiga, Teixeira-Dias, Kedzierewicz, Sousa, & Maincent, 1996). The powder XRD patterns of DM-β-CD, quinestrol, their physical mixture, and the inclusion complex are shown in Fig. 4. The XRD pattern of DM-β-CD shows three broad peaks in the 10–30° (2θ) range, thus confirming the amorphous character of this compound

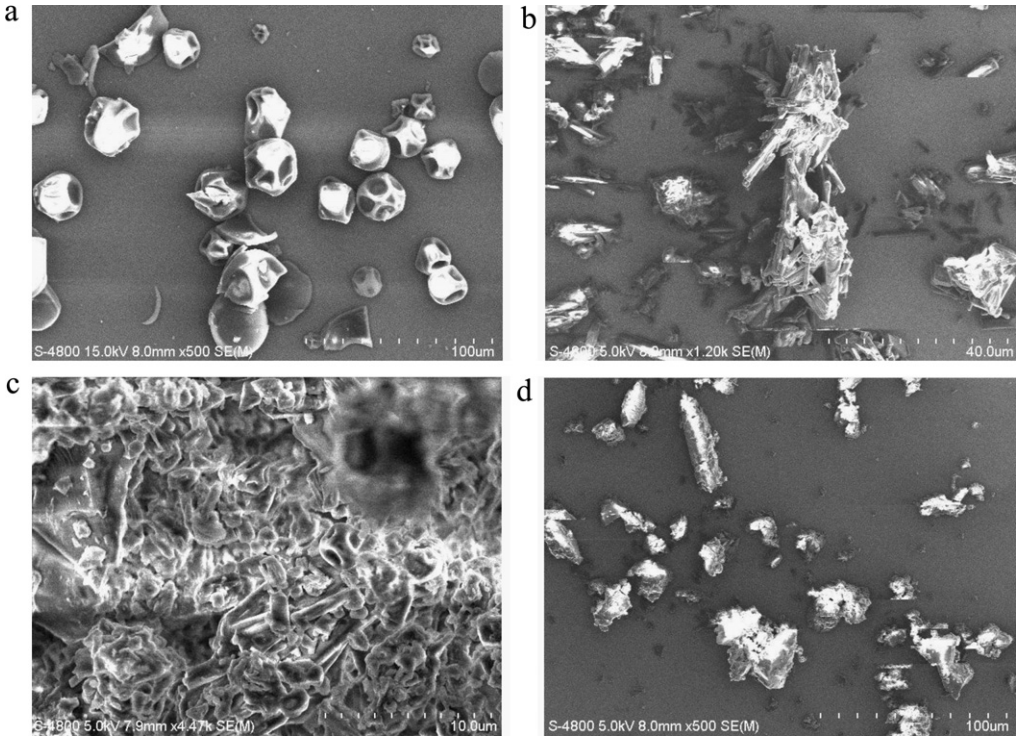

Fig. 5. Scanning electron microscopy (SEM) images of (a) DM-β-CD, (b) quinestrol, (c) physical mixture of quinestrol and DM-β-CD (1:1 molar ratio), and (d) quinestrol and DM-β-CD inclusion complex (1:1 molar ratio).

(Fig. 4a). Meanwhile, the XRD pattern of quinestrol shows intense, sharp peaks at 2θ of 13.8°, 16.3°, 17.3°, 19.5°, 21.4°, and 22.7°, as well as several minor peaks at 12.0°, 15.5°, 18.0°, 23.5°, and 25.1°. These peaks confirm the crystalline nature of the compound (Fig. 4b). The XRD pattern of the quinestrol and DM-β-CD physical mixture (Fig. 4c) is simply the superposition of the patterns of amorphous DM-β-CD and crystalline quinestrol. However, the inclusion complex of quinestrol and DM-β-CD gave a large, broad background under the crystalline peaks (Fig. 4d). The pattern is similar to that of the amorphous DM -β-CD and does not exhibit the characteristic peaks of quinestrol. This result indicates the formation of a new kind of amorphous material.

3.2.6. SEM analysis

SEM is a qualitative method used to study the structural aspects of raw materials such as CDs and drugs, or of the products obtained by different methods of preparation such as physical mixing, solution complexation, and coevaporation (de Araujo et al., 2008; Duchêne, 1987). The surface morphology of the powders, namely, DM-β-CD, quinestrol, their physical mixture, and their inclusion complex was determined using SEM. Fig. 5a shows that DM-β-CD exists as a spherical crystal containing cavity structures similar to shrinking balls. However, quinestrol (Fig. 5b) exists as a typical needle-like crystal. The structural characteristics of the physical mixture of quinestrol and DM-β-CD (Fig. 5c) show some similarities with those of the two isolated molecules. By contrast, the inclusion complex of quinestrol and DM-β-CD (Fig. 5d) appeared as irregular particles. In this complex, the original morphologies of both components disappeared, and the sizes and shapes of quinestrol and DM-β-CD changed.

A comparison of these images shows that the inclusion complex is structurally distinct not only from the free components, but also from the physical mixture of quinestrol and DM-β-CD. These results confirm the formation of the quinestrol and DM-β-CD inclusion complex.

3.2.7. ^1H and 2D NMR analysis

NMR spectroscopy is one of the most powerful tools for the study of inclusion chemistry in a solution. The information provided by the chemical shifts has been used to establish inclusion modes (Jiang et al., 2007; Kwon et al., 2009). The chemical shifts of the hydrogen atoms in the interior of the CD cavity (H-3 and H-5) become shielded and generally show a significant upfield shift in the presence of a guest molecule, whereas the hydrogen atoms on the outer surface (H-1, H-2, and H-4) are not affected or experience only a marginal shift upon complexation (Chen et al., 2011; Ge et al., 2011; Onnainty, Longhi, & Granero, 2011).

To investigate the possible inclusion mode of the quinestrol and DM-β-CD complex, the ^1H NMR spectra of DM-β-CD both in the absence and presence of quinestrol in D_2O were compared (Fig. 6a and b). The protons of quinestrol showed distinct changes in the presence of DM-β-CD, especially for the H-3 and H-5 protons, suggesting that quinestrol was inserted into the cavity.

NOESY experiments are generally performed to determine the geometry of the inclusion complexes of organic molecules with CDs (Kemelbekov et al., 2011). Two protons that are closely located in space can produce a nuclear Overhauser effect cross-correlation in NOESY or ROESY. To gain additional conformational information, the 2D NOESY of the inclusion complex of quinestrol with DM-β-CD was obtained. The NOESY spectrum of the quinestrol and DM-β-CD complex (Fig. 6c) shows appreciable cross-correlations between the H-15 of quinestrol and

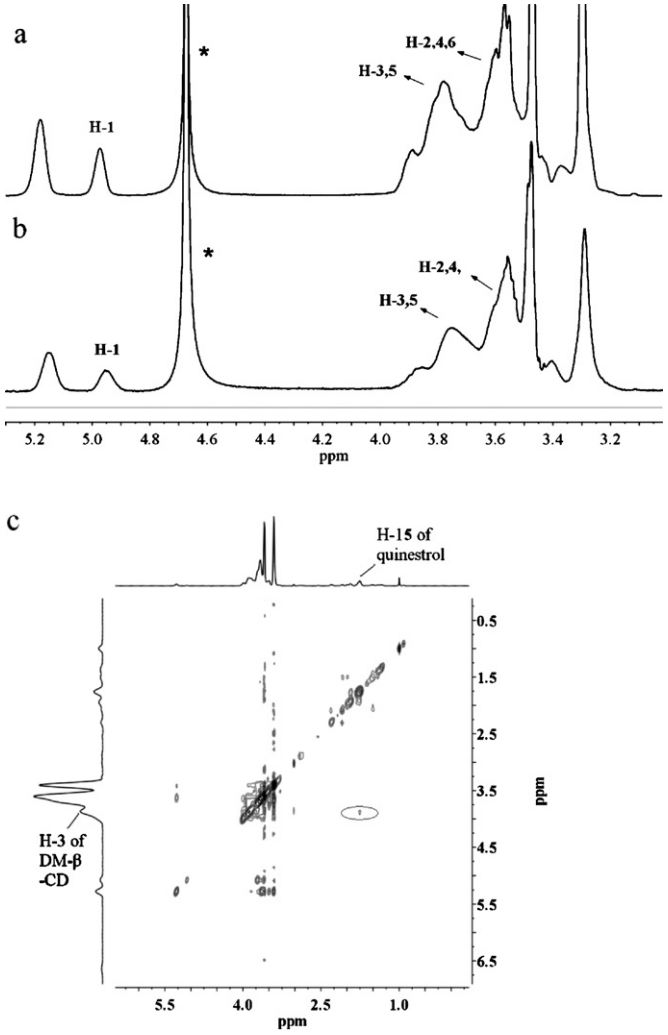

Fig. 6. Proton nuclear magnetic resonance (^1H NMR) spectra of DM-β-CD in the absence and presence of quinestrol in D_2O at 25 °C, respectively: (a) DM-β-CD, (b) the inclusion complex of quinestrol and DM-β-CD ("*" highlights the water peak). (c) Nuclear Overhauser effect spectroscopy (NOESY) pattern in D_2O at 25 °C of the inclusion complex of quinestrol and DM-β-CD.

the H-3 protons of DM-β-CD. These results indicate that the hydroxyl end of quinestrol was included into the DM-β-CD cavity.

3.3. Molecular modeling studies

Docking predicts the preferred orientation of one molecule to a second molecule when these are bound to each other to form a stable complex (Lengauer & Rarey, 1996). Molecular modeling of the DM-β-CD and quinestrol interactions was performed to determine the most probable conformation of the complex as well as to provide a visual three-dimensional profile of the complex. Docking studies and energy calculation were also conducted. To gain an insight into the binding modes and observe the changes from a different perspective, simulations of the inclusion complexes of DM-β-CD with quinestrol in three different orientations were performed. The complex 3D mode results (Fig. 7) indicate that the DM-β-CD cavity contained hydroxy and ethynyl ends. This finding is consistent with the FT-IR and NMR results. Furthermore, the distances between quinestrol and the DM-β-CD protons were calculated. Fig. 7(d) shows that the shortest distances between quinestrol and H-3 and H-5 are 2.004 and

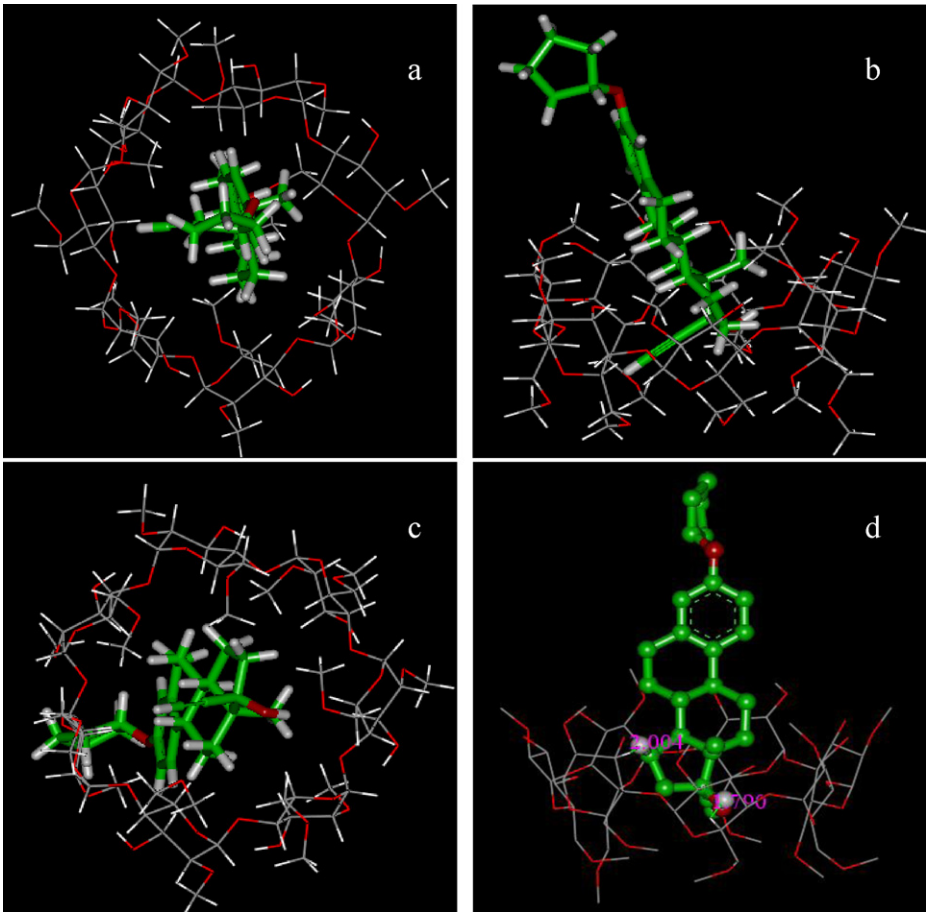

Fig. 7. Modes for the inclusion complex of quinestrol and DM-β-CD as obtained using docking calculations at different orientations: from (a) top, (b) side, (c) bottom, and (d) the nearest distance between the protons of quinestrol and DM-β-CD.

1.790, respectively. This result is consistent with that of the 2D NMR.

The enthalpy of formation of the possible complex is −27.16 kJ/mol, as calculated using Eq. (2). The ΔH values indicate that the complex is stable in water. Thus, the docking studies show that quinestrol interacted with DM-β-CD in one binding mode.

4. Conclusions

The inclusion complexation behavior, characteristics, molecular modeling, and solubilization of quinestrol with DM-β-CD were investigated. First, the inclusion complex of quinestrol with DM-β-CD was prepared. The stoichiometry was confirmed by elemental analysis, clearly indicating that an inclusion complex of quinestrol with DM-β-CD with a 1:1 molar ratio can be prepared using the solution-ultrasonic method. Second, the UV–vis, FT-IR, DSC, XRD, and SEM results show that the inclusion complex has different physicochemical characteristics from free quinestrol. In addition, several parts of quinestrol were inserted into the DM-β-CD cavity. The stability also deteriorated after the inclusion complexation. Third, ^{1}H NMR and NOESY experiments show that the hydroxyl terminal of quinestrol was encapsulated within the DM-β-CD cavity. Furthermore, molecular modeling studies, including molecular docking and energy calculations, were performed to construct a three-dimensional model of the complex and verify the experimental results. In summary, the water solubility of quinestrol was significantly improved by complexation with DM-β-CD. This inclusion complexation is a promising strategy for improving the applicability of quinestrol in agriculture and rat control in order to maintain the ecological balance and protect the environment.

Acknowledgments

This work was supported by the National Nature Science Foundation of China (31000858), the Foundation of Institute of Plant Protection (1610142012009) and the basic research special fund operations (1610122012003).

References

Alcaro, S., Ventura, C. A., Paolino, D., Battaglia, D., Ortuso, F., Cattel, L., et al. (2002). Preparation, characterization, molecular modeling and In vitroactivity of paclitaxel–cyclodextrin complexes. *Bioorganic & Medicinal Chemistry Letters*, *12*, 1637–1641.

Chen, W., Yang, L. J., Ma, S. X., Yang, X. D., Fan, B. M., & Lin, J. (2011). Crassicauline A/β-cyclodextrin host–guest system: Preparation, characterization, inclusion mode, solubilization and stability. *Carbohydrate Polymers*, *84*, 1321–1328.

Correia, I., Bezzenine, N., Ronzani, N., Platzer, N., Beloeil, J. C., & Doan, B. T. J. (2002). Study of inclusion complexes of acridine with β- and (2 6-di-O-methyl)-β-cyclodextrin by use of solubility diagrams and NMR spectroscopy. *Journal of Physical Organic Chemistry*, *15*, 647–659.

de Araujo, D. R., Tsuneda, S. S., Cereda, C. M. S., Carvalho, F. D. G. F., Preté, P. S. C., Fernandes, S. A., et al. (2008). Development and pharmacological evaluation of ropivacaine-2-hydroxypropyl-β-cyclodextrin inclusion complex. *European Journal of Pharmaceutical Sciences*, *33*, 60–71.

de Jesus, M. B., de Matos Alves Pinto, L., Fraceto, L. F., Takahata, Y., Lino, A. C. S., Jaime, C., et al. (2006). Theoretical and experimental study of a praziquantel and β-cyclodextrin inclusion complex using molecular mechanic calculations and ^{1}H-nuclear magnetic resonance. *Journal of Pharmaceutical and Biomedical Analysis*, *41*, 1428–1432.

Duchêne, D. (1987). *Cyclodextrins and their industrial uses* (pp. 131–172). Paris: Editions de Santé.

Ge, X., He, J., Yang, Y., Qi, F. M., Huang, Z., Lu, R. H., et al. (2011). Study on inclusion complexation between plant growth regulator 6-benzylaminopurine and b-cyclodextrin: Preparation, characterization and molecular modeling. *Journal of Molecular Structure*, *994*, 163–169.

Glide. (2009). Version 5.5, *Schröinger*, LLC, New York, NY.

He, J., Deng, L., & Yang, S. S. (2008). Synthesis and characterization of beta-cyclodextrin inclusion complex containing di(8-hydroxyquinoline) magnesium. *Spectrochimica Acta. Part A, Molecular and Biomolecular Spectroscopy*, *70*, 878–883.

Higuchi, T., & Connors, K. A. (1965). Phase solubility techniques. *Advances in Analytical Chemistry and Instrumentation*, *4*, 117–212.

Jiang, H. M., Sun, H. J., Zhang, S. B., Hua, R. N., Xu, Y. M., Jin, S. B., et al. (2007). NMR investigations of inclusion complexes between β-cyclodextrin and naphthalene/anthraquinone derivatives. *Journal of Inclusion Phenomena and Macrocyclic Chemistry*, *58*, 133–138.

Karathanos, V. T., Mourtzinos, I., Yannakopoulou, K., & Andrikopoulos, N. K. (2007). Study of the solubility, antioxidant activity and structure of inclusion complex of vanillin with β-cyclodextrin. *Food Chemistry*, *101*, 652–658.

Kemelbekov, U., Luo, Y., Orynbekova, Z., Rustembekov, Zh., Haag, R., Saenger, W., et al. (2011). IR, UV and NMR studies of β-cyclodextrin inclusion complexes of kazcaine and prosidol bases. *Journal of Inclusion Phenomena and Macrocyclic Chemistry*, *69*, 181–190.

Kroc, R. L., & Mischler, T. W. (1972). *Quinestrol as a rodent control agent*. United States Patent, US3655889.

Kwon, S., Lee, W., Shin, H. J., Yoon, S., Kim, Y., Kim, Y. J., et al. (2009). Characterization of cyclodextrin complexes of camostat mesylate by ESI mass spectrometry and NMR spectroscopy. *Journal of Molecular Structure*, *938*, 192–197.

Lauro, M. R., Carbone, C., Auditore, R., Musumeci, T., Santagati, N. A., Aquino, R. P., et al. (2012). A new inclusion complex of amlodipine besylate and soluble β-cyclodextrin polymer: Preparation, characterization and dissolution profile. *Journal of Inclusion Phenomena and Macrocyclic Chemistry, Online First*™.

Lengauer, T., & Rarey, M. (1996). Computational methods for biomolecular docking. *Current Opinion in Structural Biology*, *6*, 402–406.

Liang, H. C., Huo, X. F., Wang, D., Shi, D. Z., Zhang, H. Q., & Liang, J. J. (2006). A preliminary study on the control effect of a sterilant on the population of clawed gerbil. *Plant Protection*, *32*, 45–48.

Liu, Y., & Chen, Y. (2006). Cooperative binding and multiple recognition by bridged bis(β-cyclodextrin) s with functional linkers. *Accounts of Chemical Research*, *39*, 681–691.

Liu, M., Qu, J. P., Yang, M., Wang, Z. L., Wang, Y. L., Zhang, Y. M., et al. (2012). Effects of quinestrol and levonorgestrel on populations of plateau pikas Ochotona curzoniae, in the Qinghai-Tibetan Plateau. *Pest Management Science*, *68*, 592–601.

Loftsson, T., Hreinsdóttir, D., & Másson, M. (2005). Evaluation of cyclodextrin solubilization of drugs. *International Journal of Pharmaceutics*, *302*, 18–28.

MacroModel. (2009). Version 9.7, *Schröinger*, LLC, New York, NY.

Maestro. (2009). Version 9.0, *Schröinger*, LLC, New York, NY.

Marsh, R. E., & Howard, W. E. (1970). Chemosterilants as an approach to rodent control. In R. H. Dana (Ed.), *Proceedings of the fourth vertebrate pest conference, El Rancho Hotel West Sacramento, California, US* California Vertebrate Pest Committee, (pp. 55–63).

Meylan, W. M., Howard, P. H., & Boethling, R. S. (1996). Improved method for estimating water solubility from octanol/water partition coefficient. *Environmental Toxicology and Chemistry*, *15*, 100–106.

Miecznik, P., & Kaczmarek, M. (2007). Ultrasonic investigations of inclusion complexation of α-cyclodextrin by iodide ions in pseudo-binary aqueous system. *Journal of Molecular Liquids*, *133*, 120–124.

Misiuk, W., & Zalewska, M. (2009). Investigation of inclusion complex of trazodone hydrochloride with hydroxypropyl-β-cyclodextrin. *Carbohydrate Polymers*, *77*, 482–488.

Onnainty, R., Longhi, M. R., & Granero, G. E. (2011). Complex formation of chlorhexidine gluconate with hydroxypropyl-β-cyclodextrin (HPβCD) by proton nuclear magnetic resonance spectroscopy (^{1}H NMR). *Carbohydrate Research*, *346*, 1037–1046.

Pérez-Cruz, F., Jullian, C., Rodriguez, J., Arán, V. J., & Olea-Azar, C. (2009). Molecular encapsulation of 5-nitroindazole derivatives in 2,6-dimethyl-β-cyclodextrin: Electrochemical and spectroscopic studies. *Bioorganic & Medicinal Chemistry*, *17*, 4604–4611.

Rajabi, O., Tayyari, F., Salari, R., & Tayyari, S. F. (2008). Study of interaction of spironolactone with hydroxypropyl-β-cyclodextrin in aqueous solution and in solid state. *Journal of Molecular Structure*, *878*, 78–83.

Singleton, G. R., Leirs, H., Hinds, L. A., & Zhang, Z. (1999). Ecologically based management of rodent pests: Re-evaluating our approach to an old problem. In R. H. Dana, G. R. Singleton, L. A. Hinds, H. Leirs, & Z. Zhang (Eds.), *Ecologically based management of rodent pests* (pp. 17–29). Canberra: Australian Centre for International Agricultural Research.

Tang, T., Li, P. L., Luo, L. X., Shi, Z., Li, J. Q., & Cao, Y. S. (2010). Development and validation of a HPLC method for determination of levonorgestrel and quinestrol in rat plasma. *Biomedical Chromatography*, *24*, 706–710.

Veiga, F., Teixeira-Dias, J. J. C., Kedzierewicz, F., Sousa, A., & Maincent, P. (1996). Inclusion complexation of tolbutamide with β-cyclodextrin and hydroxypropyl-β-cyclodextrin. *International Journal of Pharmaceutics*, *129*, 63–71.

Ventura, C. A., Giannone, I., Musumeci, T., Pignatello, R., Ragni, L., Landolfi, C., et al. (2006). Physico-chemical characterization of disoxaril-dimethyl-β-cyclodextrin inclusion complex and in vitro permeation studies. *European Journal of Medicinal Chemistry*, *41*, 233–240.

Villaverde, J., Morillo, E., Perez-Martinez, J. I., Gines, J. M., Maqueda, C., & Agric, J. (2004). Preparation and characterization of inclusion complex of norflurazon and beta-cyclodextrin to improve herbicide formulations. *Journal of Agricultural and Food Chemistry*, *52*, 864–869.

Wang, J., Cao, Y. P., Sun, B. G., & Wang, C. T. (2011). Characterisation of inclusion complex of trans-ferulic acid and hydroxypropyl-β-cyclodextrin. *Food Chemistry*, *124*, 1069–1075.

Wang, D. W., Liu, Q., Liu, M., & Liu, X. H. (2011). The preparation, characterization and ultraviolet photodegradation of LNG-HP-β-CD. *Spectroscopy and Spectra Analysis*, *31*, 808–811.

Wu, H., Liang, H., Yuan, Q., Wang, T., & Yan, X. (2010). Preparation and stability investigation of the inclusion complex of sulforaphane with hydroxypropyl-β-cyclodextrin. *Carbohydrate Polymers*, *82*, 613–617.

Yang, B., Lin, J., Chen, Y., & Liu, Y. (2009). Artemether/hydroxypropyl-β-cyclodextrin host–guest system: Characterization, phase-solubility and inclusion mode. *Bioorganic and Medicinal Chemistry*, *17*, 6311–6317.

Zhang, Z. B., Liao, L. F., Wang, S. Q., Cao, X. P., Wang, F. S., Wang, C., et al. (2004). Effect of a contraceptive compound (EP-1) on fertility of female Brandt's voles, gray hamsters and mid-day gerbils. *Acta Zoologica Sinica*, *50*, 341–347.

Zhao, M. R., Liu, M., Li, D., Wan, X. R., Hinds, L. A., Wang, Y. L., et al. (2007). Antifertility effect of levonorgestrel and quinestrol in Brandt's voles (*Lasiopodomys brandtii*). *Integrative Zoology*, *2*, 260–268.